Progress In Electromagnetics Research M, Vol. 36, 177–183, 2014

Variations in Non-Linearity in Vertical Distribution of Microwave Radio Refractivity

Adekunle T. Adediji[1, *] and Samuel T. Ogunjo[2]

Abstract—Radio refractivity values obtained for different heights (Ground surface, 50 m, 100 m and 150 m) over a tropical station, Akure, South-Western Nigeria using in-situ data over a period of five years has been investigated for chaos. Several chaos quantifiers such as entropy, Lyapunov exponent, recurrence plot were used. Determinism was detected in the time series studied at all the levels. Results obtained from the computation of radio refractivity show that the value of radio refractivity decreases with increasing altitude while chaotic quantifiers obtained at ground level and height 100 m are found to be more chaotic than the other two levels (50 m and 150 m).

1. INTRODUCTION

A chaotic system is a deterministic system in which small changes in the initial conditions may lead to completely different behaviour later. Signal from the chaotic system is often, at first sight, indistinguishable from a random process, despite being driven by deterministic dynamics [20]. Chaos allows scientists to see order in processes that were thought to be completely random.

The unpredictability of weather and its parameters has necessitated studies on chaos in weather conditions and parameters [3, 8, 10, 14, 15, 19, 21–23]. Radio refractivity is an important parameter in the determination of the quality of UHF, VHF, and SHF signals [2]. In characterizing a radio channel, surface (ground level) and elevated refractivity data are often required, and in particular, the surface refractivity is very useful for the prediction of some propagation effects. Local coverage and statistics of refractivity, such as refractivity gradient, provide the most useful indication of the likely occurrence of refractivity related effects required for prediction methods [25].

There are, in principle, two possibilities for the determination of radio refractivity [2, 27]. These are the direct method (using refractometers) and indirect method (fixed measuring method using TV tower, Radiosonde measurement, Remote sensing techniques, Statistical and deterministic model). Whichever method is used, the measurement of the refractive index with good accuracy is difficult, because a measurement of the refractivity with an accuracy of $1N$-unit implies a relative accuracy of 10^{-6}. The precision required for meteorological studies is not so high, and routine meteorological data are therefore not well adapted to radio meteorology. Refractivity obtained by indirect method depends on air temperature, atmospheric pressure and water vapour pressure. These atmospheric parameters have been shown to decrease with increasing height under normal atmospheric conditions [6].

Previous study on this subject in Akure, Nigeria was limited to investigating chaos in surface radio refractivity [15]. The present study is aimed at investigating how chaotic quantifiers such as Lyapunov exponent, entropy, Kaplan Yorke dimension and recurrence plots affect the distribution of radio refractivity over Akure, Nigeria from the ground surface to a height of 150 m altitude and at 50 m interval. A positive Lyapunov exponent indicates that past values of refractivity at a particular level can only predict future values to a very small extent. It is essential to investigate nonlinearity in

Received 16 April 2014, Accepted 28 May 2014, Scheduled 12 June 2014

* Corresponding author: Adekunle Titus Adediji (kunleadediji2002@yahoo.co.uk).

[1] Department of Physics, The Federal University of Technology, Akure, Ondo State, Nigeria. [2] Condensed Matter and Statistical Physics Research Group, Department of Physics, Federal University of Technology, Akure, Ondo State, Nigeria.

refractivity at various levels to better understand the dynamics and for efficient prediction algorithms. The best level will be one with very low Lyapunov exponent as it is easier to predict, and the influence of external parameters on signals at that level is limited.

2. INSTRUMENTATION AND SCOPE OF DATA

Data used for this study was obtained from the on-going measurement of some weather parameters by the Radio Propagation Research Group of the Department of Physics, Federal University of Technology Akure. The measurement is in collaboration with University of Bonn, Germany and the National Space Research Development Agency (NASRDA), Nigeria. The measurement of weather parameters was made using Davis 6162 Wireless Vantage Pro2 equipped with the integrated sensor Suite (ISS), a solar panel (with an alternative battery source) and the wireless console. The fixed measuring method by a high tower was employed for the measurement with the ISSs positioned on the ground surface (0 m) and at different heights 50 m, 100 m and 150 m, respectively on the tower for continuous measurement of the weather variables. More detailed description of the instrumentation set-up and experimental site are available in [1, 26]. The data collected were those of atmospheric pressure, temperature and relative humidity which are relevant for the computation of radio refractivity and cover a five year period, from January 2007 to December 2011. Daily averages of hourly variations of the meteorological parameters for each day were obtained while the missing values were filtered.

3. METHODS

Radio refractivity, N, is given as [2, 28]

$$N = N_{dry} + N_{wet} = \frac{77.6}{T}\left(P + 4810\frac{e}{T}\right) \tag{1}$$

where P is the atmospheric pressure (hPa), e the water vapour pressure (hPa), and T the temperature (K). The water vapour pressure e is calculated from the relative humidity, H (%) and temperature, t (°C) as

$$e = H \times \frac{6.1121\exp(\frac{17.502t}{t+24097})}{100} \tag{2}$$

4. RESULTS AND DISCUSSION

The radio refractivity was computed by employing Equations (1) and (2) for the four different heights (0 m, 50 m, 100 m, and 150 m). The results were subjected to analysis using chaotic quantifiers such

Table 1. Annual variation of computed mean, minimum and maximum values of radio refractivity N (N-units) for years 2007–2011 in Akure, Nigeria.

Level (m)	Statistical properties	2007	2008	2009	2010	2011
0	Mean	366.62	360.12	366.25	363.62	363.72
	Minimum	300.55	322.24	345.91	342.35	327.56
	Maximum	387.25	371.91	373.99	374.52	375.97
50	Mean	358.54	357.63	365.55	366.89	361.15
	Minimum	302.09	319.10	347.76	346.49	326.44
	Maximum	370.29	369.71	372.37	375.03	371.25
100	Mean	357.23	357.05	361.59	365.58	360.24
	Minimum	303.19	317.16	351.40	345.17	325.77
	Maximum	368.99	368.92	374.11	374.11	370.58
150	Mean	352.22	351.57	362.34	361.28	360.35
	Minimum	298.38	310.09	344.09	343.21	323.97
	Maximum	365.19	366.24	369.95	373.63	371.87

as embedding dimension, time delay, Lyapunov exponent, Kaplan-Yorke dimension, recurrence plot, nonlinear prediction error and entropy. The methods and results obtained are discussed in the following subsections.

4.1. Variation of Radio Refractivity

Table 1 gives the summary of annual variation of radio refractivity computed for various heights across the entire period of this report. It is deduced that the value of radio refractivity decreases with increasing altitude from years 2007–2009. In 2010, the surface value was deduced to be lower than that at 50 m altitude. Also, in 2011, the value at 50 m level is lower than that at 100 m level. This anomaly might be due to the occurrence of temperature inversion at those levels.

5. PHASE SPACE RECONSTRUCTION

The refractivity data is a one dimensional time series of the form $N = x_1, x_2, \ldots, x_n$. A better understanding of the dynamics of the system is obtained in many dimensions. To reveal the multidimensional aspect of the system, phase space reconstruction of the time series is required. The space of independent variables of a set of differential equations or difference equation is called phase space or state space. To recreate the phase space of the time series $x(t_0)$, $x(t_1)$, $\ldots$, $x(t_n)$, it is extended to a phase type of m dimensions phase space with time delay tau.

$$x = \begin{pmatrix} x(t_o) & x(t_1) & x(t_i) & x(t_n + (m-1)\tau) \\ x(t_o + \tau) & x(t_1 + \tau) & x(t_i + \tau) & x(t_n + (m-2)\tau) \\ \vdots & \vdots & \vdots & \vdots \\ x(t_o + m(m-1)\tau & x(t_1 + (m-1)\tau) & x(t_1 + (m-1)\tau) & x(t_n) \end{pmatrix} \tag{3}$$

A phase space consists of several phase points. Each row in Equation (5) constitutes a phase point in a phase space. Every phase point has m weights and embodies a certain instantaneous state, and the point's trajectory of phase space is composed of the link-line of phase points. Thus the system dynamics can be studied in more dimensions in phase space. Optimal embedding dimension and time delay are critical for the best time series reconstruction. Methods available are discussed in the following subsections.

5.1. Embedding Dimension

Given a point $p(i)$ in the m-dimensional embedding space, one has to find a neighbor $p(j)$, so that $\|p(i) - p(j)\| < \varepsilon$, where $\| \ldots \|$ is the square norm and ε a small constant usually not larger than the standard deviation of the data [12, 13]. The normalized distance R_i between the $(m+1)$th embedding coordinate of points $p(i)$ and $p(j)$ is calculated using the expression

$$R_i = \frac{|x_{i+m\tau} - x_{j+m\tau}|}{\|p(i) - p(j)\|} \tag{4}$$

If R_i is larger than a given threshold R_{tr}, then $p(i)$ is marked as having a false nearest neighbor. The process is applied to all embedding dimensions, m. The dimension for which the lowest value is obtained is generally chosen as the optimal embedding dimension. This dimension prescribes the minimum number of autonomous first-order ordinary differential equations with which the time series can be modeled.

Using the method of False Nearest Neighbor, the embedding dimension for the four (4) levels were estimated (Figure 1). From the figure, there is a marked minimum at dimension $m = 4$; hence, this value was used throughout this paper. This implies that at least the refractivity can best be described in terms of four autonomous first order differential equations.

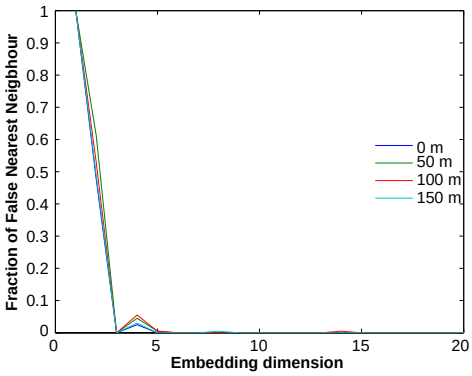

Figure 1. The false nearest neighbors fractions as a function of embedding dimension.

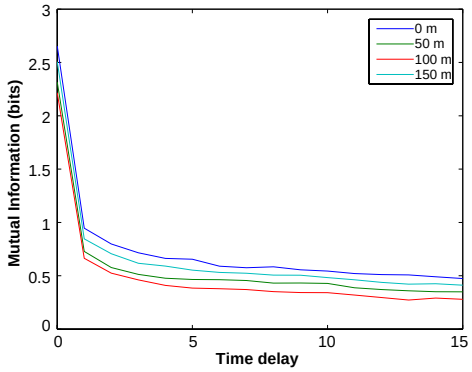

Figure 2. Mutual information as a function of timelags.

5.2. Time Delay

Two commonly used approaches to obtaining the best time delay are: autocorrelation function and mutual information [7]. The average mutual information is defined as,

$$I(\tau) = \sum_{X(i),X(i+\tau)} P(X(i), X(i+\tau)) \log_2 \left[\frac{P(X(i), X(i+\tau))}{P(X(i))P(X(i+\tau))} \right] \tag{5}$$

where i is total number of samples. $P(X(i))$ and $P(X(i+\tau))$ are individual probabilities for the measurements of $X(i)$ and $X(i+\tau)$. $P(X(i),\ X(i+\tau))$ are the joint probability densities for measurements $P(X(i))$ and $P(X(i+\tau))$. The appropriate time delay τ is defined as the first minimum of the average mutual information $I(\tau)$.

The sample autocorrelation of a scalar time series $x(t)$ of N measurements is;

$$\rho(T) = \frac{\sum_{n=1}^{N}(X_{n+T} - \hat{y})(y_n - \hat{y})}{\sum_{n=1}^{N}(y_n - \hat{y})^2} \tag{6}$$

where $\hat{y} = \frac{1}{N}\sum_{n=1}^{N} \hat{y}$ is the sample mean. The smallest positive value of T for which $\rho(T) \leq 0$ is often used as embedding lag. Data which exhibits a strong periodic component suggests a value for which the successive co-ordinates of the embedded data will be virtually uncorrelated whilst still being temporally close. The plot of mutual information against time delay is displayed in Figure 2. The value of $\tau = 2$ was chosen as the optimal time delay. The reconstructed phase space using the values obtained from time delay and embedding dimension is presented in Figure 3. An inconclusive test for chaos is the distribution of phase space. A chaotic system will have phase space localized while for periodic or noise signals, the entire phase space will be occupied.

6. LYAPUNOV EXPONENT

Lyapunov exponents (λ) quantify the exponential divergence of initially close state-space trajectories and estimate the amount of chaos. It is a measure of the rate of attraction to or repulsion from a fixed point in state space. The existence of a positive Lyapunov exponent is an evidence of a chaotic system. A system with more than one positive Lyapunov exponent is termed hyperchaotic. There are a few algorithms for the computation of the Lyapunov exponent of a time series [16–18]. In this study, we implement the Sano and Sawada algorithm for computing the Lyapunov spectrum. For an m-dimensional time series, there exist $\lambda_1, \lambda_2, \ldots, \lambda_m$ Lyapunov exponents. When sorted in descending order, λ_1 is the largest or maximal Lyapunov exponent.

$$\lambda_1 = \lim_{r\to\infty} \frac{1}{t} \ln \left(\frac{\Delta x(t)}{\Delta x(0)} \right) \tag{7}$$

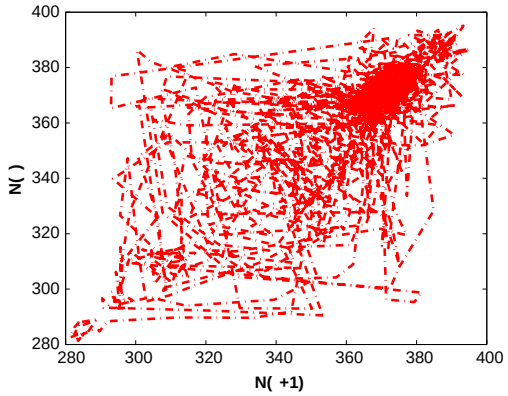

Figure 3. Phase space representation of radio refractivity for $\tau = 3$ and embedding dimension is 4.

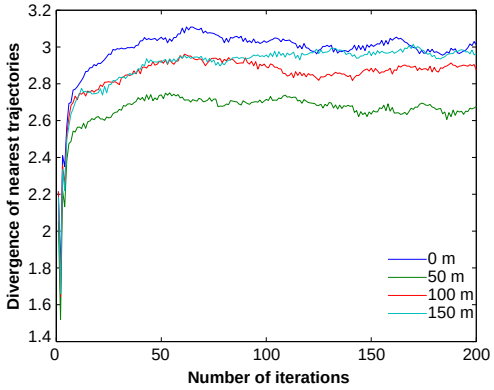

Figure 4. Divergence of trajectories as a function of trajectories.

Table 2. Values of Lyapunov exponents and Kaplan-Yorke dimension for radio refractivity at different heights.

Level (m)	λ_1	λ_2	λ_3	$\sum \lambda_i$	Kaplan-Yorke Dimension
0	0.0406	−0.3087	−0.7728	−1.0409	1.13
50	0.0472	−0.2993	−0.8759	−1.1280	1.16
100	0.0247	−0.2620	−0.7894	−1.0267	1.09
150	0.0447	-0.2708	−0.8130	−1.0391	1.17

Consequence of the Lyapunov spectrum is the Kaplan-Yorke dimension [11], and it correlates well with correlation dimension of a system. The Lyapunov spectrum and Kaplan Yorke dimension were implemented using the TISEAN package [9].

Table 2 shows the values of Lyapunov exponents and Kaplan Yorke dimension obtained from the simulations while Figure 4 shows the divergence of the trajectories at various heights. At all heights, there existed at least one positive Lyapunov exponent while the sums of the exponents were negative. This result is typical of determinism in a time series. The Lyapunov exponents were the greatest at height 50 m followed by heights at 150 m, 0 m and 100 m, respectively. We will say that the Kaplan Yorke dimension for heights 50 m and 150 m are very close, indicating similar dynamics at the heights. The patterns at other heights are the same as that of the Lyapunov exponents.

7. ENTROPY

Shannon entropy is a measure of uncertainty of a random variable. It is expressed in [4] as

$$H(X) = -k \sum_{x \epsilon \Re} p(x) \log p(x) \tag{8}$$

where $H(x)$ is the Shannon entropy and $p(x)$ the probability mass function. Entropy gives an estimate about the uncertainty coming from the "random" aspect of the dynamics. It measures the rate of increase in dynamical complexity as the system evolves with time. The computed values of Shannon entropy are presented in Figure 5. The pattern seen in the Kaplan Yorke dimension is once again exhibited with levels 50 m and 150 m having almost the same entropy followed by height 0 m and finally 100 m.

8. RECURRENCE PLOT

The technique of recurrence plot for the observation of chaotic series was proposed in [5]. It involves the computation of the $N \times N$ matrix

$$R_{i,j} = \Theta(\varepsilon_i) - \|\vec{x}_i - \vec{x}_j\| \tag{9}$$

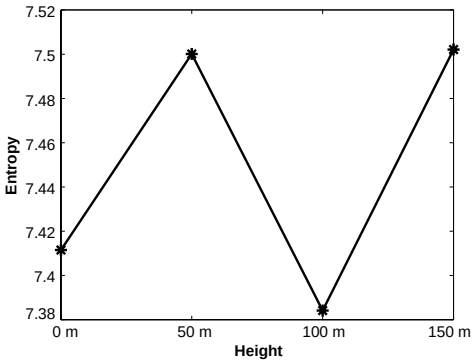

Figure 5. Entropies for the various heights.

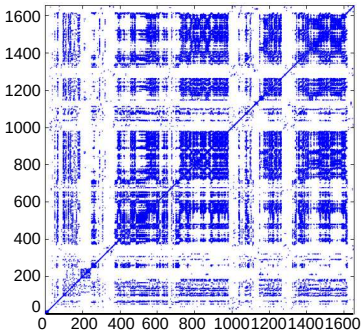

Figure 6. Recurrence plot for refractivity at height of 0 m.

where ε_i is a state dependent cut-off distance. $\|\ldots\|$ is the norm of vectors, and Θ is the Heaviside function and N the number of states. The concept of recurrence plot has been extended by Zbilut and Webber [24] to produce measures (Recurrence Quantification Analysis, RQA) from the plot and its properties. Using recurrence plots, one can graphically detect hidden patterns and structural changes in data or see similarities in patterns across the time series under study. If the time series is truly random and has no structure, the distribution of patterns/colours over the recurrence plot will be uniform and has no identifiable patterns. On the other hand, if there is some determinism in the signal generator, it can be detected by some characteristic, distinct distribution of colours/pattern. The recurrence plot of refractivity at height 0 m is computed and presented in Figure 6. The results indicate determinism in the refractivity at this height. Similar results (not shown) were obtained for the other heights.

9. CONCLUSION

Chaos has been investigated in radio refractivity over Akure, Southwestern Nigeria using quantifiers such as Lyapunov exponents, Kaplan-Yorke dimension, entropy and recurrence plot. From the results, the obtained determinism is evident in radio refractivity at all levels but with varying degree. At ground level and height 100 m, the values obtained will make the prediction horizon shorter, a result which we attribute to higher temperature and temperature/humidity inversion at ground and 100 m, respectively. Further research can be carried out using other chaos quantifiers such as recurrence quantification analysis, correlation dimension and correlation integral. Spectral analysis, wavelet transform and other signal transformation tools can also be used to further investigate radio refractivity at all levels.

From the results (entropy, Kaplan Yorke dimension and Largest Lyapunov Exponent) reported, it can be seen that values obtained at 100 m are the lowest followed by values at ground level. At ground level, the effects of surface temperature and reflected solar radiation might be responsible for the characteristic values obtained while temperature and humidity inversion could be responsible for the unique result obtained at 100 m. The significance of these results are shorter prediction time and less disorder.

REFERENCES

1. Adediji, A. T. and M. O. Ajewole, "Vertical profile of radio refractivity gradient in Akure South-West Nigeria," *Progress In Electromagnetics Research C*, Vol. 4, 157–168, 2008.
2. Bean, B. R. and E. J. Dutton, *Radio Meteorology*, Dover Publication Co., New York, 1968.
3. Campanharo, A. S. L. O., F. M. Ramos, E. E. N. Macau, and R. R. Rosa, M. J. A. Bolzan, and L. D. A. Sa, "Searching chaos and coherent structures in the atmospheric turbulence above the Amazon forest," *Phil. Trans. R. Soc. A*, Vol. 366, 579–589, 2008.
4. Cover, T. M. and J. A. Thomas, *Elements of Information Theory*, John Wiley and Sons, Inc., New York, 1991.

5. Eckmann, J. P., S. O. Kamphorst, and D. Ruelle, "Recurrence Plots of dynamical systems," *Europhysics Letters*, Vol. 5, 973–977, 1987.
6. Falodun, S. E. and M. O. Ajewole, "Radio refractive index in the lowest 100-m layer of the troposphere in Akure, South Western Nigeria," *Journal of Atmospheric and Solar-Terrestrial Physics*, Vol. 68, No. 2, 236–243, 2006.
7. Fraser, A. M. and H. L. Swinney, "Independent coordinates for strange attractors from mutual information," *Physical Review A*, Vol. 33, No. 2, 1134–1140, 1986.
8. Gallego, M. C., J. A. Garcia, and M. L. Cancillo, "Characterization of atmospheric turbulence by dynamical systems techniques," *Bound. Lay. Meteorol.*, Vol. 100, 375–392, 2001.
9. Hegger, R., H. Kantz, and T. Schreiber, "Practical implementation of nonlinear time series methods: The TISEAN package," *Chaos: An Interdisciplinary Journal of Nonlinear Science*, Vol. 9, No. 2, 413–435, 1999.
10. Henderson, H. W. and R. Wells, "Obtaining attractor dimensions from meteorological time series," *Adv. Geophys.*, Vol. 30, 205–237, 1988.
11. Kaplan, J. L. and J. A. Yorke, "Chaotic behavior of multidimensional difference equations," *Lect. Notes Math.*, Vol. 730, 204–227, 1979.
12. Kennel, M. B., R. Brown, and H. D. I. Abarbanel, "Determining embedding dimension for phase space reconstruction using a geometrical construction," *Physical Review A*, Vol. 45, 3403–3411, 1992.
13. Kodba, S., M. Perc, and M. Marhl, "Detecting chaos from a time series," *Eur. J. Phys.*, Vol. 26, 205–215, 2005.
14. Lorenz, E. N., "Deterministic nonperiodic flow," *J. Atmos. Sci.*, Vol. 20, 130–141, 1963.
15. Ogunjo, S. T., J. S. Ojo, A. T. Adediji, K. D. Adedayo, and J. B. Dada, "Chaos in radio refractivity over Akure, South-Western Nigeria," *Book of Proceedings of the 5th National Annual Conference of the Nigerian Union of Radio Science (NURS)*, 59–63, 2013.
16. Rosenstein, M. T., J. J. Collins, and C. J. De Luca, "A practical method for calculating largest Lyapunov exponents from small data sets," *Physica D*, Vol. 65 117–134, 1993.
17. Wolf, A. S., J. B. Swift, H. L. Swinney, and J. A. Vastano, "Determining Lyapunov exponents from a short time series," *Physica D*, Vol. 16, 285–317, 1985.
18. Sano, M. and Y. Sawada, "Measurement of the Lyapunov spectrum from a chaotic time series," *Phys. Rev. Lett.*, Vol. 55, 1082, 1985.
19. Siek, M. and D. P. Solomatine, "Nonlinear chaotic model for predicting storm surges," *Nonlin. Processes Geophys.*, Vol. 17, 405–420, 2010.
20. Strogatz, S. H., *Nonlinear Dynamics and Chaos*, Addison-Wesley, Reading, 1994.
21. Tsonis, A. A. and J. B. Elsner, "Chaos, strange attractors and weather," *Bull. Amer. Meteor. Soc.*, Vol. 70, 14–23, 1989.
22. Waelbroeck, H., "Deterministic chaos in tropical atmospheric dynamics," *J. Atmos. Sci.*, Vol. 52, No. 13, 2404–2415, 1995.
23. Li, X., F. Hu, and G. Liu, "Characteristics of chaotic attractors in atmospheric boundary layer turbulence," *Bound. Lay. Meteorol.* Vol. 99, 335–345, 2001.
24. Zbilut, J. P. and C. L. Webber, Jr., "Embeddings and delays as derived from quantification of recurrence plots," *Physics Letters A*, Vol. 171, 199–203, 1992.
25. Adediji, A. T., M. O. Ajewole, and S. E. Falodun, "Distribution of radio refractivity gradient and effective earth radius factor (k-factor) over Akure, South Western Nigeria," *Journal of Atmospheric and Solar-Terrestrial Physics*, Vol. 73, 2300–2304, 2011.
26. Adediji, A. T., M. O. Ajewole, S. E. Falodun, and O. R. Oladosu, "Radio refractivity Measurement at 150 m altitude on TV tower in Akure, South West Nigeria," *Journal of Engineering and Applied Sciences*, Vol. 2 1308–1313, 2007.
27. Segal, B., "Measurement of tropospheric refractive index relevant to the study of anomalous microwave propagation — Review and recommendations," CRC Report No. 1387, 1985.
28. ITU-R, "The refractive index: Its formula and refractivity data," 453-10, 2012.